

## Optimization of thermal conductivity and lightweight properties of clay bricks

Savas Ozturk

*Manisa Celal Bayar University, Department of Metallurgical and Materials Engineering, Manisa 45140, Turkey*



### ARTICLE INFO

**Keywords:**  
 Fired bricks  
 Thermal conductivity  
 Compressive strength  
 Neuro-regression

### ABSTRACT

As the demand for energy increases worldwide, the construction industry, one of the most energy-intensive sectors, requires lightweight and high-thermal-performance materials. To address this, a multi-objective optimization approach was used in this study to identify the most suitable solutions for producing strength-fired clay bricks with low thermal conductivity. Porous bricks were produced with organic waste additives to illustrate the relationship between compressive strength and thermal conductivity. A 3-factor and 3-stage Box-Behnken experimental design was utilized, with a pore-forming additive ratio (0–10% by weight of pine nut shells), firing temperature (850–1050 °C), and firing time (2–6 h) as the variables. The fired bricks' physical, mechanical, and thermal properties were determined using standard analysis methods. The bricks' compressive strength and thermal conductivity functions were generated using neuro-regression systematics. Multiple targets were defined, including minimizing the thermal conductivity and maximizing the compressive strength of the bricks. The genetic algorithm was employed to identify Pareto-optimal solutions, and the final sets of low thermal conductive-strength brick production were chosen based on these solutions. Two sets were proposed to achieve the lowest thermal conductivity, and the results confirmed the validity and feasibility of the optimization study.

### 1. Introduction

Over the past two decades, the global population has grown by 27%, projected to increase by 30% over the next thirty years [1]. As a result, the energy demand for heating and cooling in developed cities where 57% of the population lives has increased. Existing buildings typically lose approximately half of their indoor heat to the outdoors. To address this issue, lightweight insulation materials with low thermal conductivity (TC) are a popular solution to improve building energy efficiency. Thus, incorporating lightweight construction elements with low TC into building design is critical to achieving high energy efficiency [2,3].

Low-intensity building materials such as hollow clay brick and foam concrete are well-known for their excellent insulation and thermal performance due to the air spaces that prevent heat flow through the wall by conduction [2]. Closed pores can also be created as an alternative to vertical holes for creating an air space in hollow or clinker clay bricks, which can be achieved by adding pore-forming organic and inorganic additives before firing [4,5]. Using additives in bricks reduces the amount of clay consumed while improving the physicomechanical properties of the brick. Sustainability is a crucial factor in selecting additives for the construction industry. Sustainable raw materials such as fly ash, waste marble, rice husk ash, waste glass, metal slags, rice husk, waste pomace, olive mill waste, tea waste, and wood sawdust have

been reported in the literature to improve the TC and compressive strength (CS) of bricks, depending on the additive ratio and firing conditions [3,6–17]. Recent studies on brick production that have investigated different types of organic and inorganic additives, experimental variables, targets, and optimal results are presented in Table 1.

Bricks can be produced with various pore-forming additives, such as hazelnut shell, palm shell, and walnut shell, which help in the sintering behavior of the brick during combustion, reducing both the sintering temperature and time [4,5]. In this regard, pine nutshell (PNS) is also a suitable alternative additive to facilitate brick sintering. In 2022, global pine nut production (kernel basis) has reached a total of 46,330 metric tons [19]. As part of the agricultural processing of pinecones, an approximate yield of 13–20 g of pine nuts and 45–55 g of PNS is obtained. Based on the pine nut/shell ratio, an estimated total of about 150,000 metric tons of PNS can be inferred. The PNS, denoted as a smokeless fuel source [20], combusts with minimal residue (1.7% ash content) [21] and yields high calorific value (4912 Kcal/kg) [22]. This makes combustion a widely preferred method for the disposal of organic waste containing PNS due to its favorable characteristics. Some studies have focused on evaluating PNS using it as activated carbon [23], as supercapacitor electrode material [24], as biomass [25], as anode material for Na-ion batteries [26], and in Chromium(VI) adsorption [27]. The chemical composition of PNS ash predominantly consists of high

<https://doi.org/10.1016/j.jestch.2023.101566>

Received 30 June 2023; Received in revised form 22 August 2023; Accepted 30 October 2023

2215-0986/© 2023 Karabuk University. Publishing services by Elsevier B.V. This is an open access article under the CC BY license (<http://creativecommons.org/licenses/by/4.0/>).

**Table 1**  
Recent studies on brick productions.

Additives	Variables	Objectives	Optimum Results
Iron mine waste [12]	Firing time, firing temperature, particle size	Production of tailing porous bricks and industrial waste gas filter	Apparent Porosity 88.88%, CS: 0.38 MPa, TC: 0.036 W/(m·K) at 1070 °C for 3 h by 15-hour milling time
Bottom ash and fly ash [15]	Additive ratio, firing temperature	Evaluation of industrial waste in ceramic production	CS: 35.7 MPa, TC: 0.427 W/(m·K) with 30 wt% add at 950 °C
Rice husk ash [9]	Additive ratio	Mechanical and thermal characterization of earth bricks	CS: 30.3 MPa, TC: 1.25 W/(m·K) with 10 wt% add
Gypsum board [11]	Additive ratio, firing temperature	Investigation of the firing temperature and additive ratio effects on mechanical and thermal characterization of bricks	CS: 28.9 MPa, TC: 0.57 W/(m·K) with 40 wt% add. at 1050 °C
Blast furnace slag, fly ash [14]	Additive ratio, firing temperature	Evaluation of industrial waste in ceramic production	CS: 401 W: 42.4 MPa, TC: 0. / (m·K) with 40 wt% add. at 1050 °C
Sugarcane bagasse ash, rice husk ash [18]	Additive ratio	Evaluation of agricultural waste in ceramic production	CS: 5.55 MPa, TC: 0.35 W/(m·K) with 15 wt% add.
Coal and wheat husk [8]	Additive ratio	Evaluation of waste in brick production	CS: 20 MPa, TC: 0.21 W/(m·K) with 40 wt% add.
Waste micro cellulosic fiber [17]	Additive ratio	Evaluation of waste in brick production	CS: 14 MPa, TC: 0.574 W/(m·K) with 2.5 wt% add.
Tea waste [13]	Additive ratio, firing temperature	Investigation of the firing temperature and additive ratio effects on mechanical and thermal characterization of bricks	CS: 11 MPa, TC: 0.574 W/(m·K) with 10 wt% add.
Olive mill waste [7]	Additive ratio, firing temperature	Investigation of the firing temperature and additive ratio effects on mechanical and thermal characterization of bricks	CS: 16.99 MPa, TC: 0.477 W/(m·K) with 2.5 wt% add.

levels of potassium oxide, magnesium oxide, and calcium oxide, with the remaining portion comprising oxide phases of soil elements [22]. Despite the similarity in composition between the ash and clay raw material, PNS has not been employed in direct or ash-based brick production. Nevertheless, the incorporation of PNS into the clay matrix at low proportions is anticipated to result in low CO<sub>2</sub> emissions and negligible adverse environmental effects during the sintering process.

In porous brick production, the type, size, shape, thermal behavior, and proportion of the additive material determine the form and density of the resulting pores. These pore characteristics directly influence the density, TC, and CS properties of the fired clay brick [3]. Organic residues like PNS create pores within the brick structure after the combustion process, varying in size and shape based on their dimensions. Materials such as rice husk and wood chips tend to create long and slender pores, while those like palm, walnut, and hazelnut tend to generate more spherical pores [3,28]. The dimensions and densities of these pores are contingent upon the additive amount and sintering parameters. Barnabas et al. [28] incorporated walnut shell powder with dimensions below 75 µm into clay mixtures at a maximum weight fraction of 10% and fired them at 950 °C and 1100 °C for 2 h. They noted that among the bricks produced for both temperatures, only those with 10% walnut shell exhibited the lowest TC values, although they did not meet mechanical standards. Moumni et al. [29] blended argan nut shell and wheat straw with dimensions below 800 µm into clay mixtures at a maximum weight fraction of 10% and fired them at 900 °C for 2 h. They achieved the lowest TC values in bricks with individual or combined 10% weight fraction additives. However, none of the wheat straw proportions and argan nutshell proportions exceeding 5% met the standard for compressive strength.

The optimal use of waste materials in fired brick production is of great importance, and many studies have been conducted to model and optimize their performance [2,30–35]. Different methods, including Response Surface Methodology (RSM), Artificial Neural Networks (ANN), and Regression Analysis (RA), have been used to determine the effects of process parameters such as additive ratio, firing temperature, and firing time on the production of fired bricks. Optimization algorithms, such as Random Forest, LPNORM, and Fuzzy Synthetic Evaluation Algorithms, have also been employed to determine the best combination of process parameters [32,36–42]. Table 2 lists recent studies on modeling and optimization in brick production, including the types of additives, objectives, variables, modeling methods, and optimization algorithms used.

Optimizing multiple purposes has been very beneficial for engineering applications. For example, the Multi Objective Genetic Algorithm (MOGA) has been successfully applied in many construction

applications, energy and sensors. Holland developed the concept of Genetic Algorithm and his colleagues in the 1960 s and 1970 s, inspired by the evolutionist theory of the origin of species [43,44]. The evolutionist theory elucidates the natural selection process leading to the survival of adaptable species and the fading of weaker ones. Robust species pass on their genes, gradually leading to populations dominated by ideal gene combinations. Over time, slow evolution introduces random genetic changes, fostering the emergence of new species with better chances of survival. This process might result in the decline of weaker species in favor of stronger ones. The most important genetic operators that make up the Genetic Algorithm and significantly impact its performance are selection, crossover, and mutation [45]. Genetic algorithm, whose main character is internal parallelism and effective use of global information, has been used successfully in many engineering applications. One of the applications of this algorithm is to reach optimum solutions to building design problems [46–49]. Genetic algorithm has been used in building optimization studies with one or more goals such as low emission and economical green building production, low energy consumption and thermal comfort dormitory design [49], reduction of life cycle carbon footprint and cost in building renovation, reduction of energy consumption [47], reduction of external thermal load [48].

For many problems in real life and engineering applications, optimizing for a single goal can yield undesirable results for other goals. Therefore, there is a common phenomenon of combining several objective functions into a single function. However, preparing a perfect objective function that optimizes each objective simultaneously is nearly impossible. Hence, for multi-objective problems, it is better to create an acceptable range of solutions for each objective. Multi-objective evolutionary algorithms are generalized approaches to construct a Pareto optimal solution set [43,44]. The advantages of multi-objective optimization over single-objective optimization can be expressed as follows [43,50].

- Multi-objective optimization considers multiple conflicting objectives simultaneously. This approach allows for a broader exploration of the solution space.
- Unlike single-objective optimization, multi-objective optimization considers trade-offs among different objectives. This aids in identifying Pareto optimal solutions, a group of solutions optimal for various objectives.
- Multi-objective optimization provides decision-makers with deeper insights into inherent trade-offs among objectives. This empowers them to make informed choices from a range of optimal solutions.

**Table 2**

Recent studies on brick productions with modelling and optimizations.

Additives	Objectives	Variables	Modeling method	Optimization algorithm
Charcoal [40]	Production of thermal-acoustic clay bricks	Firing temperature, particle size	RA	–
Petrochemical Wastes [38] Fly ash, sugarcane bagasse ash, waste marble dust [41]	Production of clinker bricks with high heat resistance Investigation of utilization of the agro and industrial wastes for brick with acceptable compressive strength	Additive ratio Additive ratio	RA RA	– –
Plastic wastes [42]	Investigation of the usability of plastic waste in different proportions in cement brick	Additive ratio	RSM	–
Municipal solid waste, paper mill sludge, water hyacinth, paper mill sludge compost and water hyacinth compost [39]	Investigation of the effects of additives, soils, firing temperature and mixing ratio on brick performance.	Firing temperature, additive ratio, different types of soils	RA	Random Forest algorithm
Heavy clays [37]	Investigate the effect of calculated mineral content and firing temperature on compressive strength, and physical properties of bricks	Mineral content and firing temperature	ANN	LPNORM algorithm
Waste sludges, coal dust, fly and landfill ashes, soybean crust, sawdust, sunflower flakes and their ashes [32]	Investigation of the effect of adding organic and inorganic industrial waste on shaping, drying and firing of heavy clay bricks	Firing temperature, additive ratio	RSM	Fuzzy Synthetic Evaluation algorithm

- By employing multi-objective optimization, decision-makers gain enhanced insight into the trade-offs inherent in different objectives, empowering them to make well-informed decisions based on a spectrum of optimal solutions.
- Multi-objective optimization offers decision-makers a deeper understanding of trade-offs between various objectives. This approach enables informed decisions by presenting a range of optimal solutions.
- Multi-objective optimization promotes diversity within the solution space, preventing early convergence to a single solution. This method encourages the identification of a wide range of high-quality solutions by avoiding fixation on a single outcome.
- Multi-objective optimization enables the exploration of various solutions that might not be obvious in single-objective optimization by considering multiple goals. This approach fosters the development of innovative and resilient solutions by incorporating different objectives.

Clay bricks have a wide range of applications for insulation purposes. The TC properties are an essential factor that influences the insulation performance of these bricks. TC refers to how a material conducts heat, and high TC facilitates heat transfer [51]. However, the high TC values of clay bricks can adversely affect insulation performance [52]. Therefore, special design and material selection are necessary to improve the insulation properties of bricks with low TC values. In this regard, CS emerges as a significant factor. The CS of clay bricks is a critical characteristic for ensuring structural durability. As CS increases, bricks enhance their load-bearing capacity, contributing to the structural resilience [53]. In this context, using bricks for insulation purposes with both low TC values and adequate CS provides an effective solution that combines insulation performance and structural integrity.

In the literature, various additives have been employed in brick production using a similar experimental approach. In these studies, the results obtained have generally been evaluated based on their ability to meet specific brick standards. However, there has not been an experimental arrangement aimed at simultaneously optimizing multiple properties of the bricks. In this context, this study aimed to develop a genetically based design method to optimize the thermo-mechanical properties of fired clay bricks. The objective was to achieve maximum CS and minimum TC simultaneously. The multi-objective optimization process involved several steps, including determining brick production parameters using Box-Behnken design of experiment (DOE), producing and testing bricks, analyzing their physical, mechanical, and thermal properties, preparing objective functions for CS and TC using neuro-regression analysis, conducting multi-objective optimization of CS and TC simultaneously using genetic algorithms, and validating the results

through testing. This study investigates the effects of using PNS wastes as a pore forming additive in brick production on mechanical and thermal properties. It also presents the first study in the literature in this field by optimizing the multiple properties of bricks using a multi-objective optimization approach.

## 2. Experimental

### 2.1. Materials and method

Raw clay was sourced from a local brick-producing company, while PNS was obtained as a byproduct from a commercial pine nut processing factory (see Fig. 1). To eliminate physically bound water, the PNS and clay underwent an oven-drying process at 80 °C for 12 h. Subsequently, they were milled using a ring mill. After milling, both raw materials underwent sieving to achieve the desired particle size. The powders utilized in brick production had particle sizes below 150 µm, with the average particle size of PNS and clay measuring approximately 79 µm and 68 µm, respectively. The mixing and firing conditions for 17 sets of brick samples were established based on a three-factor, three-level Box-Behnken DOE design. The semi-dry mixtures were molded into 20 mm pellets under a pressure of 20 MPa. Following drying and settling, the cylindrical pellets were fired in an electric oven. The firing process of the bricks involved a two-stage heat treatment, determined based on the thermal gravimetric analysis results of the raw materials. In the first stage, the bricks were gradually heated to 600 °C at a rate of 2.5 °C/min, followed by further heating to firing temperatures of 850 °C, 950 °C and 1050 °C at a rate of 5 °C/min. For a visual representation of the experimental setup, please refer to Fig. 2.

Physical properties of fired bricks, such as bulk density (BD), apparent porosity (AP), apparent specific gravity (ASG) and water absorption (WA), were measured according to ASTM C20 [54] by Archimedes method. In addition, mechanical properties were measured by a compression testing machine (Shimadzu AGS-X) with ASTM C-67 [55] and TC was measured with the C-Therm TCI TC analyzer using a temporary plane welding method [56].

### 2.2. Box- Behnken experimental design

To investigate the impact of additive content, firing temperature, and firing time on the mechanical and thermal properties of the fired brick, a Box-Behnken DOE set was employed. The DOE set consisted of three numerical factors, namely PNS wt% ( $X_1$ ), firing temperature ( $X_2$ ), and firing time ( $X_3$ ), which were varied at low, medium, and high levels. A total of 17 experiments were conducted with five replicates at the intermediate level, resulting in a DOE matrix that incorporated the three



**Fig. 1.** Raw materials; a) raw clay, b) ground clay, c) PNS, d) ground PNS.

independent variables' three-level values (as presented in Table 3). Box-Behnken DOE methodology involves replicating the central levels of variables, which is particularly useful in identifying and homogeneity issues that may arise due to the mixed oxide content of the bricks. This aspect contributes to enhancing the reliability of the experimental study.

### 2.3. Optimization

This study aims to find optimum production parameters that minimize heat conduction and maximize CS in the same fired clay brick. A MOGA was used to optimize the two targets described above for fired clay bricks. The ratio of pore-forming additive, firing time and firing temperature are defined as three variables to be optimized for fired clay bricks.

The optimization procedure was carried out by preparing the objective functions for the TC and CS of the fired clay bricks and obtaining Pareto optimal results with MOGA. The data used to derive the objective functions were obtained from samples generated according to the Box-Behnken DOE. The data were divided into two parts according to the neuro-regression approach [57]. First, the objective functions were obtained by fitting the train data to the function in Eq. (1) by Wolfram Mathematica. The reliability of the functions was determined by calculating the Coefficient of Determination ( $R^2$ ), Root Mean Square Error (RMSE), Mean Absolute Error (MAE), Model Efficiency (ME), and limit values and the functions satisfying all the conditions for the optimization algorithms were determined as the objective functions. Finally, two objective functions were used by a MOGA by Matlab to find optimal solutions for bricks with low TC and high CS.

$$Y = a_0 + a_1 X_1 + a_2 X_2 + a_3 X_3 + a_4 X_1^2 + a_5 X_2^2 + a_6 X_3^2 + a_7 X_2 X_1 \\ + a_8 X_1 X_3 + a_9 X_2 X_3 \quad (1)$$

**Table 3**  
Variables and their experimental design levels used in Box-Behnken DOE.

Exp. Number	X <sub>1</sub>	X <sub>2</sub>	X <sub>3</sub>	PNS (wt%)	Temp. (°C)	Time (h)
1	1	0	-1	10	950	2
2	1	-1	0	10	850	4
3	1	1	0	10	1050	4
*4	0	0	0	5	950	4
5	-1	0	1	0	950	6
*6	0	0	0	5	950	4
*7	0	0	0	5	950	4
*8	0	0	0	5	950	4
9	-1	0	-1	0	950	2
10	-1	1	0	0	1050	4
11	0	-1	-1	5	850	2
12	0	1	1	5	1050	6
*13	0	0	0	5	950	4
14	0	1	-1	5	1050	2
15	1	0	1	10	950	6
16	0	-1	1	5	850	6
17	-1	-1	0	0	850	4

\* Five Replicas (Central Point of Variables).

$$RMSE = \sqrt{\frac{1}{n} \sum_{i=1}^n (X_{A,i} - X_{P,i})^2} \quad (2)$$

$$R^2 = 1 - \frac{\sum_{i=1}^n (X_{A,i} - X_{P,i})^2}{\sum_{i=1}^n X_{P,i}^2} \quad (3)$$

$$MAE = \frac{1}{n} \sum_{i=1}^n |X_{A,i} - X_{P,i}| \quad (4)$$

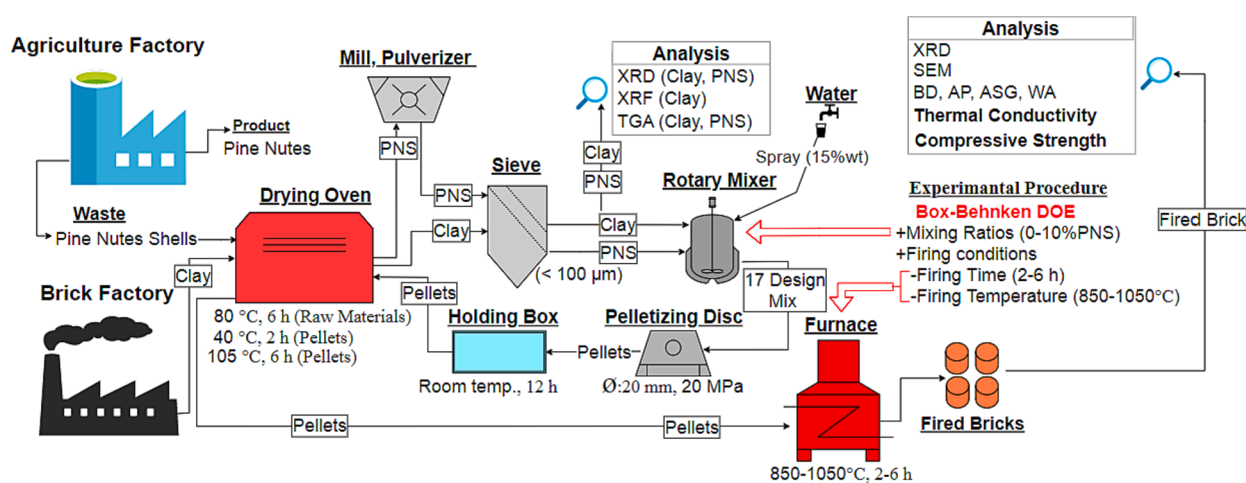


**Fig. 2.** Schematic representation of the production and testing stages of bricks.

$$ME = 1 - \frac{\sum_{i=1}^n (X_{A,i} - X_{P,i})^2}{\sum_{i=1}^n (X_{A,i} - \bar{X}_{P,i})^2} \quad (5)$$

where,  $X_A$  is actual data and  $X_P$  is predicted data.

### 3. Results and discussion

#### 3.1. Characterization of the raw materials

##### 3.1.1. X-Ray fluorescence (XRF) analysis

The chemical composition of the raw clay was determined by XRF analysis. Main oxides 60.6%  $\text{SiO}_2$ , 15.7%  $\text{Al}_2\text{O}_3$ , other oxides 6.2%  $\text{Fe}_2\text{O}_3$ , 3.1%  $\text{MgO}$ , 2.6%  $\text{CaO}$ , 2.4%  $\text{K}_2\text{O}$ , 0.8%  $\text{Na}_2\text{O}$  and 0.6  $\text{TiO}_2$  have been determined. In addition, the ignition loss was determined as 9.2% by weight. This value is the mass loss of the raw clay material during heating due to the removal of physically and chemically absorbed water and the decomposition of organic and inorganic components.

##### 3.1.2. X-ray diffraction (XRD) analysis

For crystalline phase content, the XRD patterns of clay and PNS powder are shown in Fig. 3. The clay' XRD pattern includes mainly quartz ( $\text{SiO}_2$ ), kaolinite ( $\text{Al}_2\text{Si}_2\text{O}_5(\text{OH})_4$ ), and illite ( $\text{KAl}_2[\text{Si}_3\text{AlO}_{10}] (\text{OH})_2$ ) phases. It can be a typical non-calcareous clay with high iron oxide content in mineral evaluation. XRD pattern of PNS includes cellulose phases, which peaked at  $15^\circ$ ,  $16.3^\circ$  and  $22.1^\circ$  of cellulose 1-alpha and  $14^\circ$ ,  $16.3^\circ$  and  $21.5^\circ$  of the cellulose 1-beta phase.

##### 3.1.3. Thermogravimetric analysis (TGA)

TGA of the raw materials is given in Fig. 4. The total weight change of clay up to  $900^\circ\text{C}$  is about 8%. In the derivative weight graph of the clay, it is seen that the mass loss is mostly caused by the evaporation of the physically absorbed water in the  $0\text{--}100^\circ\text{C}$  range, and then by the dehydration of the clay components in the  $580\text{--}700^\circ\text{C}$  range. In addition, four mass changes were observed in the range of  $100\text{--}580^\circ\text{C}$ , due to the removal of organic materials in the clay composition by burning. The PNS graph's mass was determined to decrease by 70% up to  $800^\circ\text{C}$ . It was observed that 10% of the mass change was due to the evaporation of physical water up to  $100^\circ\text{C}$  and 60% to the combustion of organic components such as cellulose, hemicellulose and lignin in the derivative weight graph of PNS.

#### 3.2. Physical properties of the fired bricks

Brick porosity is a crucial attribute that influences both the physico-mechanical and thermal characteristics of bricks. An increase in porosity leads to improved water absorption and thermal insulation properties,

despite reduced mechanical strength [28,58–60]. Thus, depending on the design objectives, parameters affecting porosity are optimized to achieve the desired brick characteristics. According to Eliche-Quesada et al. [61], elevating firing temperatures seals fine pores in ceramic materials and augments the liquid phase content, consequently decreasing the AP. Furthermore, an increase in the proportion of pore-forming additives also results in an increase in AP. Ozturk et al. [13] manufactured fired bricks with up to 12.5% tea waste additive at  $950^\circ\text{C}$  and  $1050^\circ\text{C}$ . They noted a 10.6% change in porosity with respect to temperature for additive-free bricks and a 6.6% change for additive-modified bricks. Sutcu et al. [7] produced fired bricks with up to 10% olive mill waste additive at  $850^\circ\text{C}$ ,  $950^\circ\text{C}$ , and  $1050^\circ\text{C}$ . They reported a 12.5% and 3.85% change in porosity for unadulterated and additive-modified bricks, respectively. Similarly, Barnabas et al. [28] incorporated up to 10% walnut shell additive at  $950^\circ\text{C}$  and  $1100^\circ\text{C}$ , yielding comparable outcomes. Moumni et al. [29] observed that increasing the firing time of clay would reduce pore size and volume. Their findings indicated a roughly 50% decrease in pore volume and a 30% decrease in pore size when the firing duration was extended from 1 to 6 h. As these literature discussions unmistakably reveal, utilizing PNS as a pore-forming agent within brick matrices, along with variations in firing temperature and duration, results in the production of porosity that directly alter the thermal performance and mechanical properties of the bricks.

Fig. 5 depicts the physical properties of fired bricks such as AP, WA, BD, and ASG obtained through the Archimedes test. The AP of fired bricks has a direct influence on their WA, BD, and thermal insulation properties. The data presented in Fig. 5a indicates that the bricks' AP increased with the percentage of PNS and decreased with the increase in firing time and temperature. The BD is determined by the amount and size of porosities present in the ceramic body. The visible porosity decreased, and BD increased with the increase in firing time and temperature. Bricks are categorized as light (< $1680\text{ kg/m}^3$ ), medium ( $1680\text{--}2000\text{ kg/m}^3$ ), or normal weight (greater than  $2000\text{ kg/m}^3$ ) according to ASTM C90 [62], and all the bricks in this study were light or medium weight. Additionally, the WA of bricks is an indicator of their resistance to environmental humidity and must meet mandatory usability requirements as per the ATSM C20 standard [54]. The WA value of the bricks used in harsh weather conditions should be between 17 and 22%, while there is no limit under normal conditions. As shown in Fig. 5c, only additive-free bricks and 5% PNS at  $1050^\circ\text{C}$  bricks meet the standard, while the rest require wall cladding. Finally, the ASG of the bricks was not significantly affected by the change in production parameters, which is consistent with previous studies that used pore formers in brick production [7,13,63].

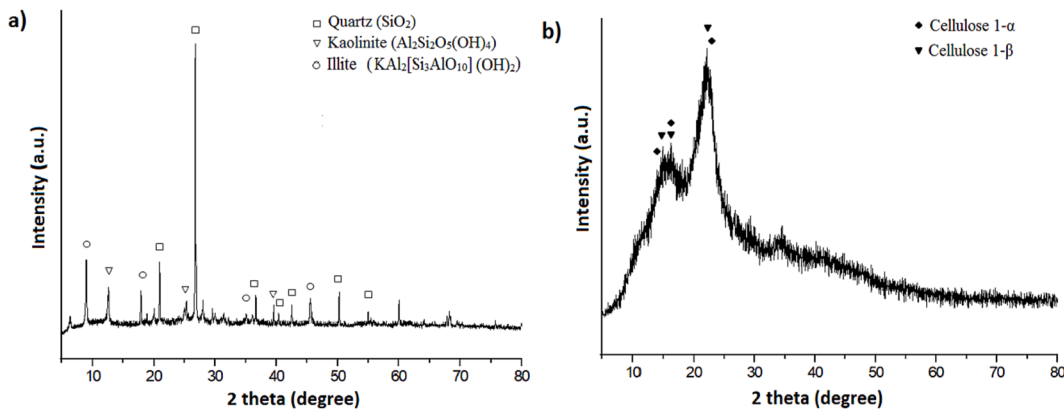


Fig. 3. XRD patterns of raw materials: (a) clay and (b) PNS.

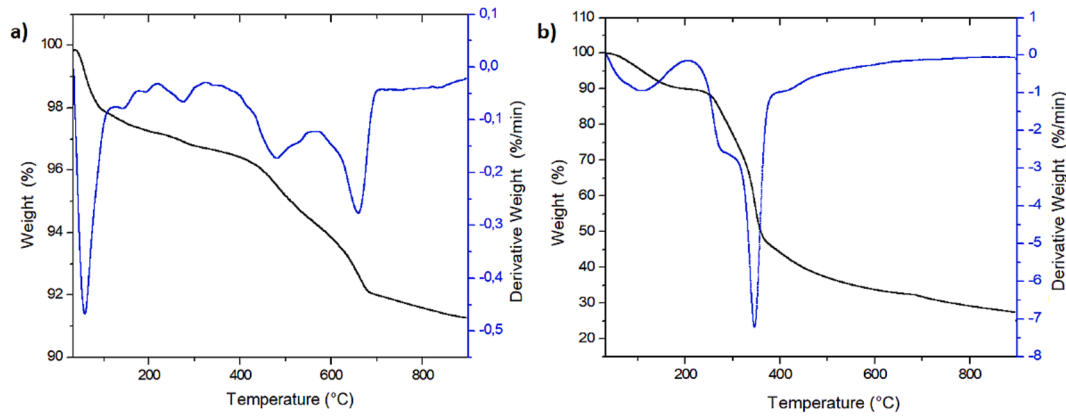


Fig. 4. TGA results of raw material: (a) clay and (b) PNS.

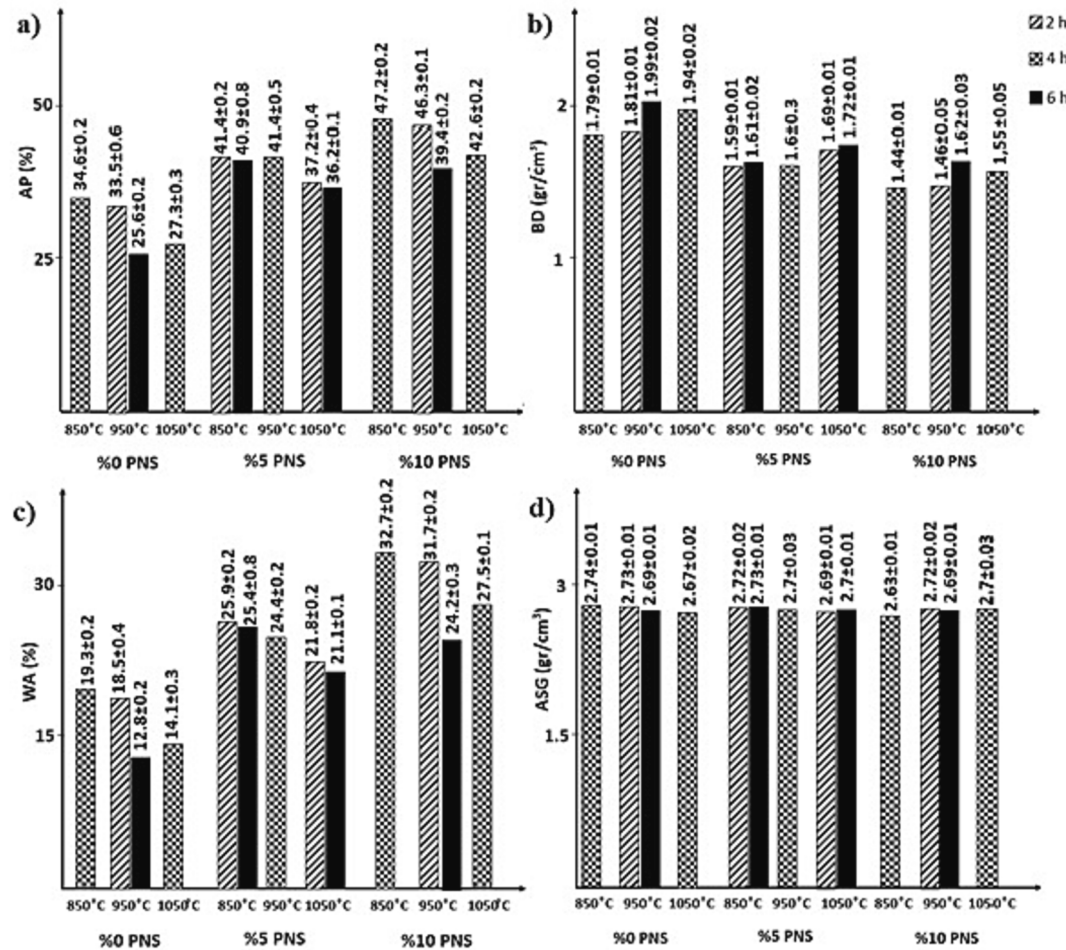


Fig. 5. Physical properties of fired bricks.

### 3.3. Microstructure and phase analysis of the fired bricks

Fig. 6 displays microstructure Scanning Electron Microscope (SEM) images of fractured surfaces of brick samples fired at 850 °C, 950 °C, and 1050 °C, magnified at 2000x. With the increase in firing temperature, it is observed that the layered structure of clay disappears, giving way to enhanced formation of a vitreous phase within the matrix. Additionally, the rise in temperature correlates with a noticeable reduction in pore size. Energy Dispersive Spectroscopy (EDX) analyses were conducted on the pores left by each pore-forming agent and from the bulk material.

Uniform elemental compositions were identified in both EDX regions for all samples. This consistency indicates that the elemental distribution of the PNS ash closely resembles the mineralogy of the brick matrix. It can be inferred that the ash contributes some elementally similar constituents (K, Si, Al) to the feldspathic phase within the brick structure.

To assist in interpreting the physical properties of the brick samples fired at different temperatures, XRD analyses were performed on the samples with the same additive ratio (see Fig. 7). The XRD patterns reveal that quartz is the main phase in all three fired brick samples. However, at 850 °C and 950 °C, hematite and muscovite phases are

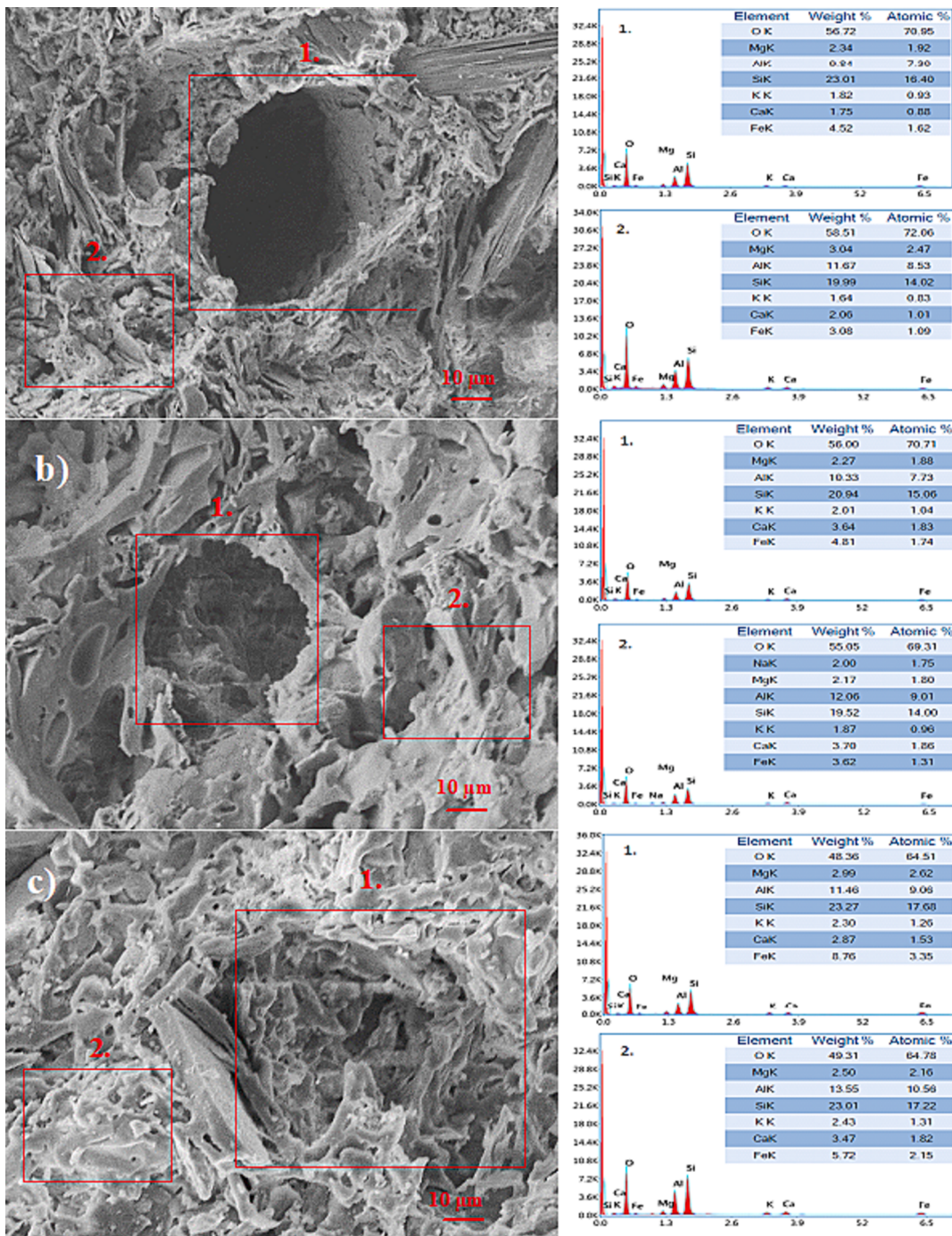


Fig. 6. SEM-EDX analysis of samples with 10% PNS at different firing temperature: a) 850 °C, b) 950 °C, and c) 1050 °C.

present, while the muscovite phase is absent at 1050 °C. Possibly, at 1050 °C, this phase might have transformed into a feldspathic phase within the brick matrix. PNS, by leaving minimal ash content at firing temperatures, generates pores within the structure. When examining the SEM images of the fractured surfaces of the bricks, no residual ash particles are observed in the pore regions left by the combustion of the PNS. This observation suggests that due to the chemical composition of the ash resembling that of fired bricks, it is inferred that the ash integrated with the clay components at elevated temperatures. In this study, both the low incorporation of PNS and its low ash content render its identification through XRD analysis unfeasible.

#### 3.4. Thermal conductivity of the fired bricks

Fig. 8 displays the average TC values of the fired bricks. These values are important for the insulation of buildings. Notably, the TC decreased by 43.57% from 0.815 to 0.459 W/mK as the additive ratio increased from 0 to 10%. The effect of firing time on TC was also investigated at three different firing temperatures. When the firing time was increased from 2 to 6 h for the samples containing 5% PNS fired at 850 and 1050 °C, the TC values decreased by 1.409% and 3.535%, respectively. The TC value of the samples containing 10% PNS added fired at 950 °C decreased by 10.773%. Furthermore, increasing the firing temperature from 850 to 1050 °C resulted in a significant decrease in the TC values for the 2 h and 6 h fired samples with 5% PNS, by 16.403% and

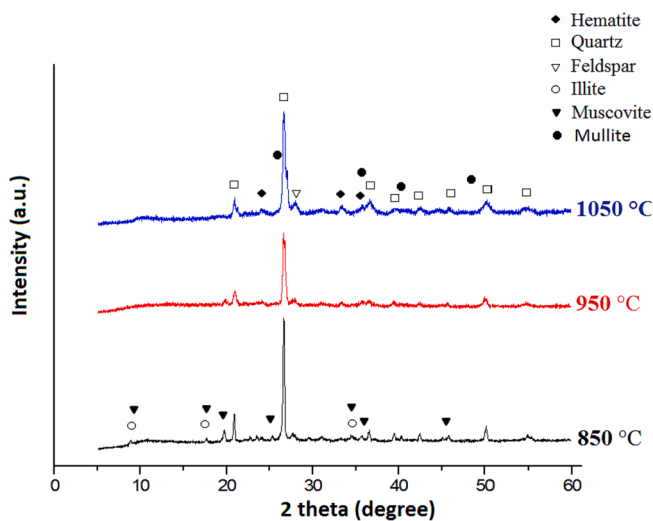


Fig. 7. XRD patterns of fired bricks fired at three firing temperatures.

18.842%, respectively. The sample with 10% PNS added and fired for 4 h decreased by 17.918%. Moreover, it was found that the TC values of the bricks were related to the AP and BD values, where an increase in porosity led to a decrease in TC. Therefore, the porosity parameters of the bricks also influenced the TC values. Incorporating organic additives at levels of 10% and above significantly enhances the AP while reducing TC. Similar outcomes have been reported in the literature for different organic residues such as tea waste [13], argan nut shell [29], olive mill waste [7], and walnut shell [28].

### 3.5. Compressive strength of the fired bricks

The CS values of the fired bricks are shown in Fig. 9. The results indicate that the CS value decreases as the amount of additive increases, which is related to the AP, BD, and TC values of the bricks. The incorporation of organic additives exceeding 10% as pore-forming agents in brick production leads to a notable reduction in CS. In a study conducted by Barnabas et al [28] using 10% walnut shell for brick manufacturing resulted in a decrease of 47.5% in CS. Similarly, Moumni et al. [29] introduced argan nut shell and wheat straw in the same proportion to the clay matrix, resulting in a significant reduction of 73.8% in CS. This considerable decrease can be attributed to the substantial dimensions of

the additive materials. In present study, the sample with 10% PNS fired at 850 °C for 4 h has a CS value of 14.2 MPa, which is higher than the minimum required CS value (> 7 MPa) depending on the BD of the fired bricks. The effect of firing time on the CS value was investigated at three different temperatures. For the additive-free brick samples fired at 950 °C, the CS value increased by 79.96% as the firing time increased from 2 h to 6 h. Similarly, for the 5% PNS sample fired at 850 °C and 1050 °C, the CS value increased by 15.11% and 26.37%, respectively, as the firing time increased from 2 h to 6 h. For the 10% PNS sample fired at 950 °C, the CS value increased by 100.502% with the increase in firing time from 2 h to 6 h. As the firing temperature increased from 850 °C to 1050 °C, the CS values increased by 95.153%, 85.49%, and 63.45% for additive-free bricks fired for 4 h, 5% PNS sample fired for 2 h, and 10% PNS sample fired for 4 h, respectively. In general, it can be concluded that the CS value increases with the increase of firing temperature and time. The CS value increased considerably with the increase of firing time at 950 °C, indicating that the muscovite/illite component in the raw clay material transformed into mullite/feldspar structure at these temperatures, which requires sufficient firing time [64,65].

### 3.6. Optimization

The proposed model functions for the two process outputs, compressive strength (Y1) and thermal conductivity (Y2), are presented using Eq. (1), without entering any coefficients. Model selection was based on the following criteria: (i)  $R^2$  values greater than 0.9 were preferred, (ii) the limitation values should not differ from the actual values by more than  $\pm 50\%$ , and (iii) RMSE, MAE, and ME values should be close to 0, 0, and 1, respectively. Fig. 10 shows the  $R_{\text{training}}^2$ ,  $R_{\text{testing}}^2$ , RMSE, MAE, ME, and limit values of the regression models for the CS and TC of the bricks.

The model selection criteria were based on  $R_{\text{training}}^2$ ,  $R_{\text{testing}}^2$ , RMSE, MAE, and ME values of the CS and TC regression models. Additionally, the difference between the predicted models and the experimental limit values was limited to less than fifty percent. The high  $R_{\text{testing}}^2$  values of 0.96 for both models indicated their reliability. Figs. 11 and 12 were generated using Y1 and Y2 functions to demonstrate the effects of firing temperature and PNS ratio on the CS and TC of the fired bricks. The response of two factors ( $X_1$ ,  $X_3$ ) were shown together in these graphs while the other factor ( $X_2$ ) was held constant.

Figs. 11 and 12 depict the estimated CS and TC of clay bricks fired at various temperatures. The results demonstrate that increasing firing temperature and time lead to an increase in CS, while an increase in the

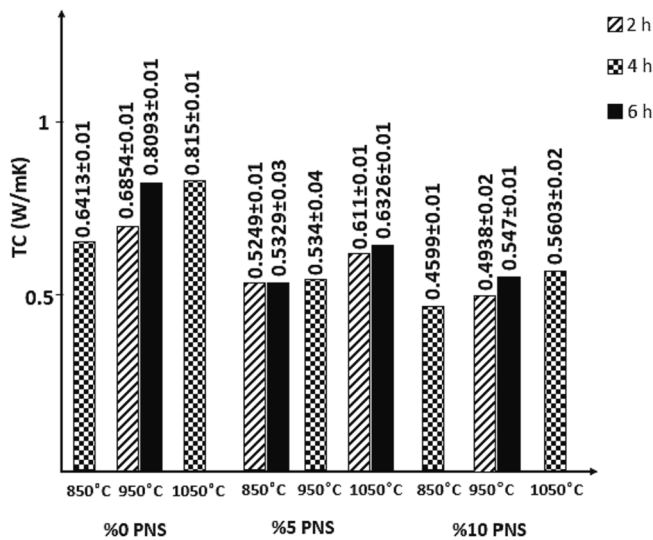


Fig. 8. Thermal conductivity of fired bricks.

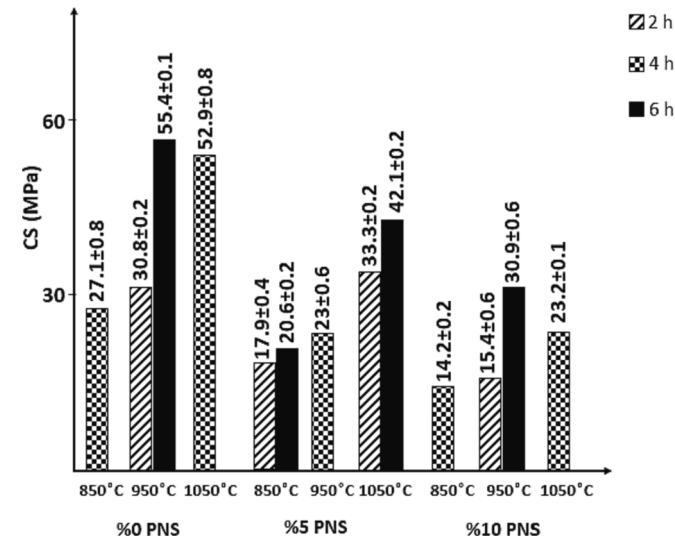


Fig. 9. Compressive strength of fired bricks.

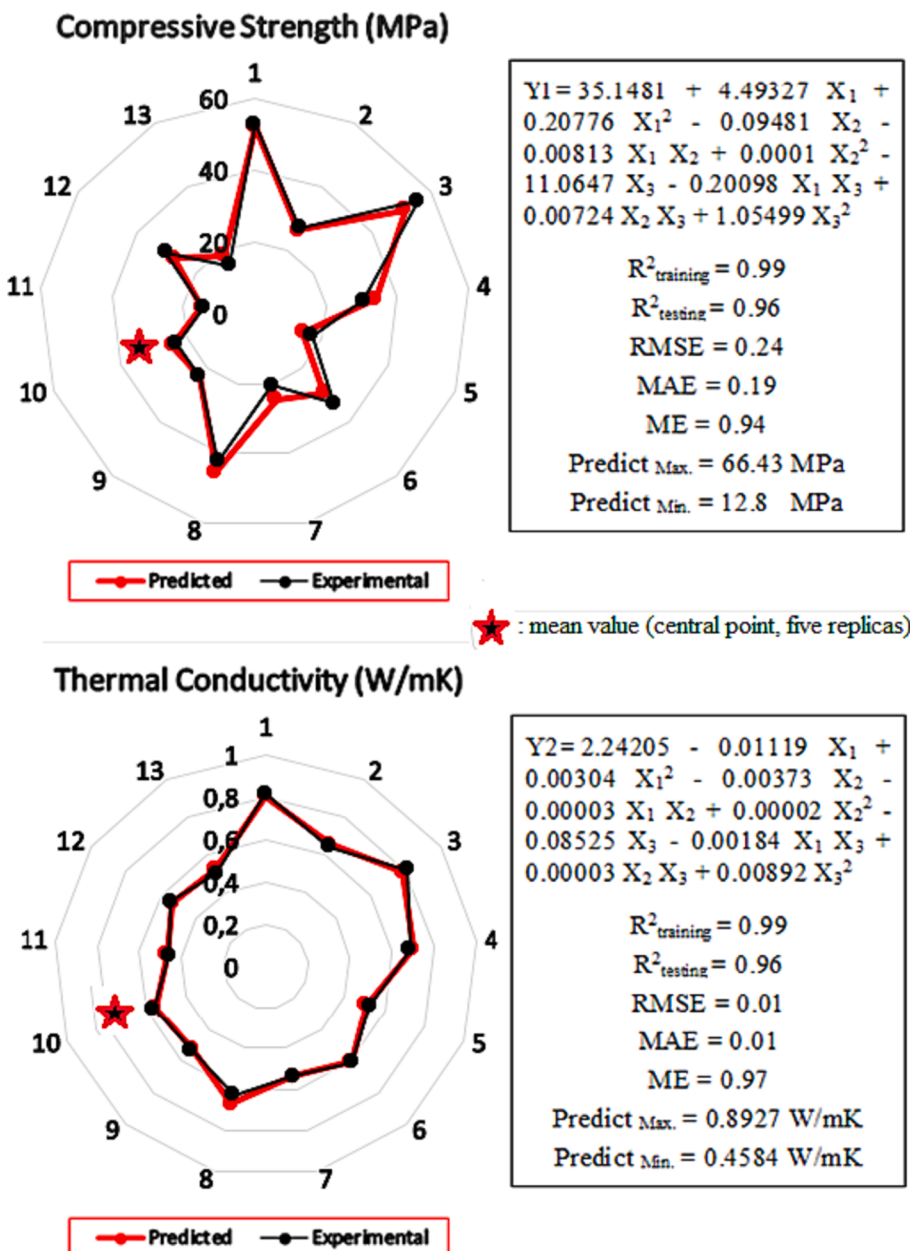


Fig. 10. Radar graphs and statistical results of CS and TC models of fired bricks.

percentage of %PNS decreases CS. The lowest CS is achieved when firing at 850 °C for 2 h with %PNS ranging from 4% to 10%. On the other hand, the highest CS has observed in additive-free bricks fired at 1050 °C for 6 h. However, CS increases for each %PNS value above 4 h. The lowest TC is observed in samples fired for 2 h with %PNS greater than 8% at all firing temperatures.

The main key parameters of the MOGA are PNS wt% ( $X_1$ ), firing temperature ( $X_2$ ), and firing time ( $X_3$ ). The limits of the objective functions were set as  $0\% < X_1 < 10\%$ ,  $850^\circ\text{C} < X_2 < 1050^\circ\text{C}$ , and  $2 \text{ h} < X_3 < 6 \text{ h}$ , which were within the experimental range. Moreover, the algorithm's design variables were real numbers, and the search space was continuous. Therefore, MATLAB was utilized to solve the multi-objective optimization problems with these constraints. In this stage, the Y1 and Y2 objective functions, as illustrated in Fig. 9, were integrated into the program. Subsequently, the multi-objective optimization tool was executed, employing the limit values of  $X_1$ ,  $X_2$ , and  $X_3$ , thus yielding the Pareto graph. The optimum values of  $X_1$ ,  $X_2$ , and  $X_3$  were obtained for the two outcomes associated with achieving the lowest TC.

These identified parameters were then utilized for further experimental investigations, during which the TC and CS of the specimens were measured. Table 4 presents the relevant options for the Genetic Algorithm.

Fig. 13 displays the Pareto front, which comprises 18 solutions attained through multi-objective optimization of the TC and CS of fired bricks. The Pareto front is modeled by a quadratic nonlinear polynomial function to investigate the relationship between the TC and CS functions. In the case of porous bricks, the TC and CS exhibit an inverse relationship with the level of porosity. This implies that as the porosity decreases, both the TC and CS of porous bricks increase. Hence, there exists a positive correlation between the TC and CS values, where an increase in one parameter is accompanied by an increase in the other. The fitting function exhibits an  $R^2$  value of 0.9598, demonstrating that the model accurately describes the relationship between the TC and CS functions. Furthermore, the Pareto results reveal that the CS exceeds 7 MPa [48], the minimum acceptable value for fired bricks, even at the lowest TC values.

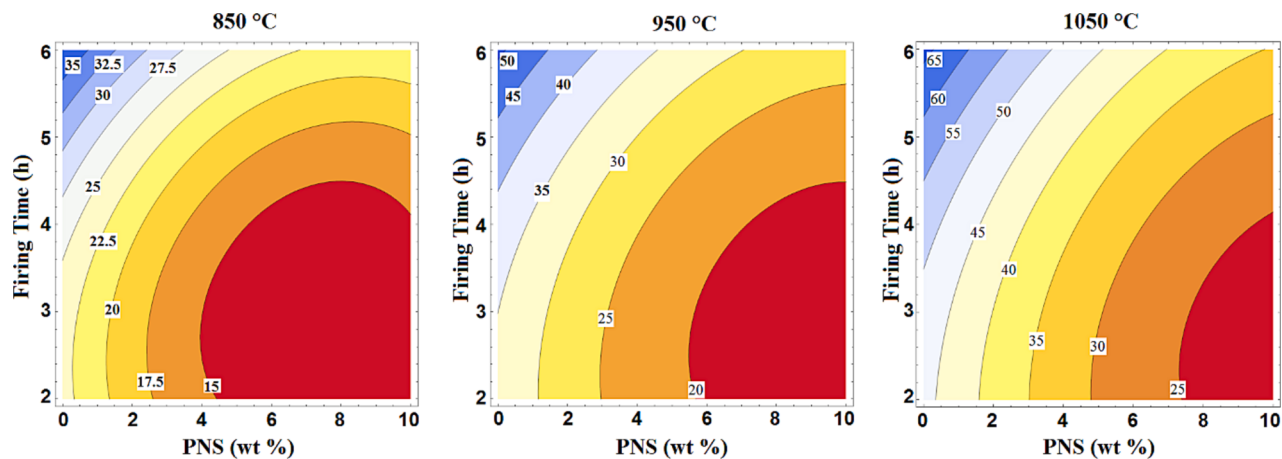


Fig. 11. Contour plots showing the effect of the % PNS and firing time on the response of compressive strength.

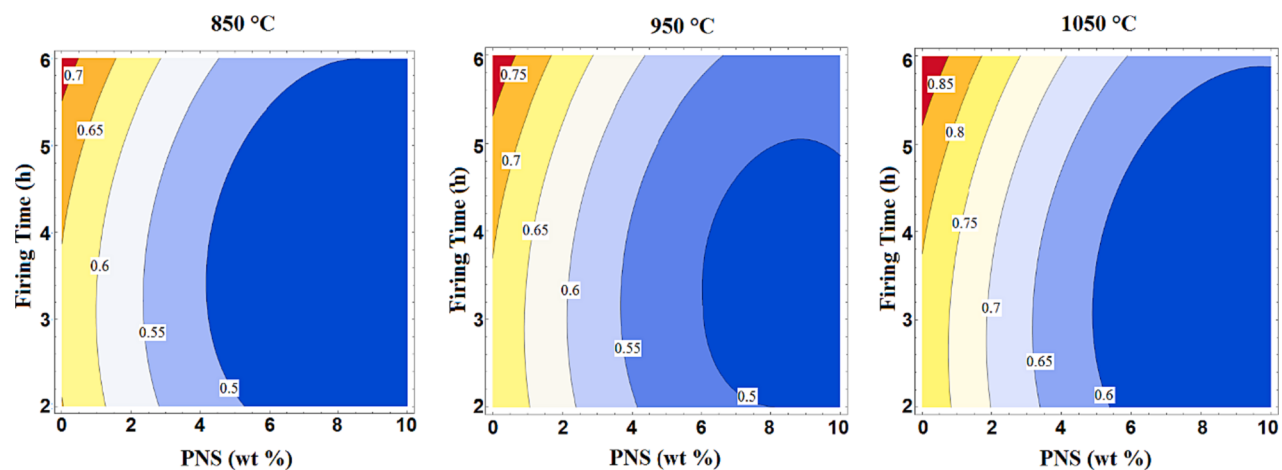


Fig. 12. Contour plots showing the effect of the % PNS and firing time on the response of thermal conductivity.

**Table 4**

The options list for the GA algorithms.

Population of individuals	50
Generations	100
Function Tolerance	$10^{-4}$
Constraint Tolerance	$10^{-3}$
Crossover Fraction	1
Pareto fraction	0.35

Comparing the two lowest TC solutions in Fig. 12, the PNS ratio changes from 7.797 % to 6.642 %, firing temperature changes from 850.325 °C to 851.824 °C and firing time changes from 3.676 h to 5.196 h, respectively. To validate the modeling and optimization, two additional confirmation experiments were performed to compare the predictions with the optimal conditions of these two results with the low TC. Optimum temperature values were rounded as integers (850 °C and 852 °C) according to the settings of the firing oven. The results of the confirmation experiments and the predicted results of the models are given in Table 5.

The confirmation experiments' results to validate the modeling and optimization show good agreement with the predicted results for both optimal values. In Confirmation 1, the experimental TC and CS results

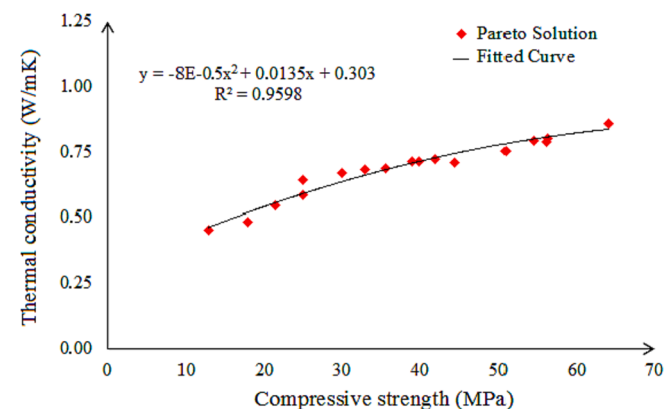


Fig. 13. Pareto solutions and fitted curve for thermal conductivity with compressive strength.

were measured as 0.4601 W/mK and 12.37 MPa, respectively. The models estimated 0.4534 W/mK and 12.8443 MPa with a difference of -1.47% and +3.83% from the experimental results. In Confirmation 2, the models estimated the results with a difference of -1.68% and -3.03%.

**Table 5**

Results of responses obtained with optimized firing parameters.

Responses	<u>Confirmation 1</u>		<u>Confirmation 2</u>	
	Predicted	Experimental	Predicted	Experimental
Thermal Conductivity (W/mK)	0.4534	0.4601	0.4833	0.4916
Compressive Strength (MPa)	12.8443	12.37	17.8715	18.43

#### 4. Conclusions

The characteristics of bricks, including their physical, thermal, and mechanical properties, can vary widely. Therefore, it is important to identify the best combination of properties for a given application. Materials are typically designed to achieve multiple targets, with varying levels of importance placed on each target. This study aimed to optimize the most critical objectives for fired clay bricks to achieve energy savings and successfully produce strong and lightweight bricks. To achieve this, the CS and TC values were determined experimentally and modeled using the neuro-regression method, then optimized using MOGA.

The article reported on the impact of firing conditions and the addition of organic waste PNS on the physical, thermal, and mechanical properties of fired clay bricks. The use of PNS as an additive resulted in bricks with lower TC but increased WA and decreased BD and CS as the PNS usage rate increased. The high WA values obtained limit the use of these bricks in harsh weather conditions, making them suitable only for cladded walls.

The utilization of PNS as a pore-forming agent has led to a reduction in both TC and CS due to its direct correlation with AP and BD. Moreover, the elevation in firing temperature of the bricks has resulted in the emergence of novel phases. This phenomenon has concurrently decreased the visible porosity while elevating the brick density. The transformation of the muscovite phase within the brick composition into another phase (amorphous or feldspathic) or its dissolution into another phase (feldspathic) at temperatures exceeding 950 °C can also be ascribed to this behavior.

Considering the produced bricks for their potential applications as load-bearing or insulation bricks, the optimal specimens for load-bearing bricks possess a CS of 55.4 MPa, achieved at 950 °C for a firing duration of 6 h. Conversely, for exclusive insulation brick production, the ideal samples are those incorporating 10% PNS, with the TC value of 0.4599 W/mK, fired at 850 °C for 2 h. The specimens that exhibit optimal characteristics in both aspects are the ones presented during the validation tests.

Regarding the modelling and optimization results, CS and TC models have been shown statistically to describe the process with high accuracy. Furthermore, the high-accuracy prediction capabilities of the models ensured success in the optimization study. In the multi-objective optimization study, many solutions have been proposed to produce strength bricks with low TC. Among the proposed designs, validation tests were performed on the two lowest TC solutions, and the success of the model predictions was proven.

The properties of fired clay bricks vary significantly and the selection of the best matches between existing and designed profiles is crucial. In this article, the most important objectives of fired clay bricks were optimized for energy saving, resulting in the production of strength-light bricks. The experimental results indicated the effects of firing parameters and different ratios of additives on brick production. The use of additive organic waste PNS resulted in lightly baked bricks with low TC, but high WA values limit their use to cladded walls in harsh weather conditions. Firing temperature affects CS values more than TC values,

while firing time affects both properties, especially at temperatures above 950 °C. The modelling and optimization results showed that the CS and TC models accurately describe the process, ensuring success in the optimization study. The validation tests on the two lowest TC solutions confirmed the success of the model predictions.

The originality of this study is the simultaneous optimization of multiple attributes of brick, a fundamental construction material. The findings obtained through such an approach are being presented for the first time in the literature through this study.

#### Declaration of Competing Interest

The authors declare that they have no known competing financial interests or personal relationships that could have appeared to influence the work reported in this paper.

#### References

- [1] U. Nations, *World population prospects 2019*. Vol (ST/ESA/SE. A/424) Department of Economic and Social Affairs: Population Division, 2019.
- [2] M. Sutcu, J.J. del Coz Diaz, F.P.A. Rabanal, O. Gencel, S. Akkurt, Thermal performance optimization of hollow clay bricks made up of paper waste, *Energ. Buildings* 75 (2014) 96–108.
- [3] R. Ruparathna, K. Hewage, R. Sadiq, Improving the energy efficiency of the existing building stock: A critical review of commercial and institutional buildings, *Renew. Sustain. Energy Rev.* 53 (2016) 1032–1045.
- [4] P. Muñoz, M. Morales, V. Letelier, and M. Mendivil, *Fired clay bricks made by adding wastes: Assessment of the impact on physical, mechanical and thermal properties*. 2016.
- [5] N. Jannat, R.L. Al-Mufti, A. Hussien, B. Abdullah, A. Cotgrave, Utilisation of nut shell wastes in brick, mortar and concrete: A review, *Constr. Build. Mater.* 293 (2021), 123546.
- [6] A. Martínez-Molina, I. Tort-Ausina, S. Cho, J.-L. Vivancos, Energy efficiency and thermal comfort in historic buildings: A review, *Renew. Sustain. Energy Rev.* 61 (2016) 70–85.
- [7] M. Sutcu, S. Ozturk, E. Yalamac, O. Gencel, Effect of olive mill waste addition on the properties of porous fired clay bricks using Taguchi method, *J. Environ. Manage.* 181 (2016) 185–192.
- [8] S. Ahmad, Y. Iqbal, R. Muhammad, Effects of coal and wheat husk additives on the physical, thermal and mechanical properties of clay bricks, *Bol. SECV* 56 (3) (2017) 131–138.
- [9] T.P. Huynh, C.L. Hwang, K.L. Lin, S.H. Ngo, Effect of residual rice husk ash on mechanical-microstructural properties and thermal conductivity of sodium-hydroxide-activated bricks, *Environ. Prog. Sustain. Energy* 37 (5) (2018) 1647–1656.
- [10] S.M.S. Kazmi, M.J. Munir, I. Patnaikuni, Y.-F. Wu, U. Fawad, Thermal performance enhancement of eco-friendly bricks incorporating agro-wastes, *Energ. Buildings* 158 (2018) 1117–1129.
- [11] K.-Y. Chiang, H.-R. Yen, C.-H. Lu, Recycled gypsum board acted as a mineral swelling agent for improving thermal conductivity characteristics in manufacturing of green lightweight building brick, *Environ. Sci. Pollut. Res.* 26 (33) (2019) 34205–34219.
- [12] R. Li, Y. Zhou, C. Li, S. Li, Z. Huang, Recycling of industrial waste iron tailings in porous bricks with low thermal conductivity, *Constr. Build. Mater.* 213 (2019) 43–50.
- [13] S. Ozturk, M. Sutcu, E. Erdogmus, O. Gencel, Influence of tea waste concentration in the physical, mechanical and thermal properties of brick clay mixtures, *Constr. Build. Mater.* 217 (2019) 592–599.
- [14] O. Surul, T. Bilir, A. Gholampour, M. Sutcu, T. Ozbaakkaloglu, O. Gencel, Recycle of ground granulated blast furnace slag and fly ash on eco-friendly brick production, *Eur. J. Environ. Civ. Eng.* (2019) 1–19.
- [15] M. Sutcu, E. Erdogmus, O. Gencel, A. Gholampour, E. Atan, T. Ozbaakkaloglu, Recycling of bottom ash and fly ash wastes in eco-friendly clay brick production, *J. Clean. Prod.* 233 (2019) 753–764.
- [16] N.H. Hoang, T. Ishigaki, R. Kubota, M. Yamada, K. Kawamoto, A review of construction and demolition waste management in Southeast Asia, *J. Mater. Cycles Waste Manage.* 22 (2) (2020) 315–325.
- [17] C. Arslan, O. Gencel, I. Borazan, M. Sutcu, E. Erdogmus, Effect of waste-based micro cellulose fiber as pore maker on characteristics of fired clay bricks, *Constr. Build. Mater.* 300 (2021), 124298.
- [18] S.M.S. Kazmi, S. Abbas, M.J. Munir, A. Khitab, Exploratory study on the effect of waste rice husk and sugarcane bagasse ashes in burnt clay bricks, *J. Build. Eng.* 7 (2016) 372–378.
- [19] International Nut & Dried Fruit Council. Nuts & Dried Fruits Statistical Yearbook; INC International Nut & Dried Fruit: Reus, Spain, 2022; Available online: <https://inc.nutfruit.org/technical-projects/> (accessed on 18 August 2023).
- [20] R. Tabakaev, K. Ibraeva, A. Astafev, Y. Dubinin, D. Altynbaeva, K. Larionov, S. Yankovsky, N. Yazykov, Pine nut shells of Siberian cedar as a resource for the high-strength smokeless fuel, *Biomass Convers. Biorefin.* (2022) 1–11.
- [21] A.U. Sen, R. Correia, A. Longo, C. Nobre, O. Alves, M. Santos, M. Gonçalves, I. Miranda, H. Pereira, Chemical composition, morphology, antioxidant, and fuel

- properties of pine nut shells within a biorefinery perspective, *Biomass Convers. Bioref.*. (2022) 1–13.
- [22] S. Batbileg, B. Purevsuren, M. Battsetseg, A. Ankhtuya, D. Batkhishig, Characterization of the Pyrolytic Products of Pine Nut Shells, *Int. J. Chem.* 11 (2) (2019) 37–49.
- [23] A.S. Mestre, R.M. Viegas, E. Mesquita, M.J. Rosa, A.P. Carvalho, Engineered pine nut shell derived activated carbons for improved removal of recalcitrant pharmaceuticals in urban wastewater treatment, *J. Hazard. Mater.* 437 (2022), 129319.
- [24] L. Qin, Z. Hou, S. Lu, S. Liu, Z. Liu, E. Jiang, Porous carbon derived from pine nut shell prepared by steam activation for supercapacitor electrode material, *Int. J. Electrochem. Sci.* 14 (9) (2019) 8907–8918.
- [25] L. Qin, Y. Wu, Z. Hou, E. Jiang, Influence of biomass components, temperature and pressure on the pyrolysis behavior and biochar properties of pine nut shells, *Bioresour. Technol.* 313 (2020), 123682.
- [26] H. Guo, K. Sun, Y. Lu, H. Wang, X. Ma, Z. Li, Y.-S. Hu, D. Chen, Hard carbons derived from pine nut shells as anode materials for Na-ion batteries, *Chin. Phys. B* 28 (6) (2019), 068203.
- [27] G. Li, J. Zhang, J. Liu, S. Chen, H. Li, Investigation of the adsorption characteristics of Cr (VI) onto fly ash, pine nut shells, and modified bentonite, *Desal. Water Treat.* 195 (2020) 389–402.
- [28] A.A. Barnabas, O.A. Balogun, A.A. Akinwande, J.F. Ogbodo, A.O. Ademati, E. I. Dongo, V. Romanovski, Reuse of walnut shell waste in the development of fired ceramic bricks, *Environ. Sci. Pollut. Res.* 30 (5) (2023) 11823–11837.
- [29] B. Moumni, M. Achik, H. Benmoussa, A. Oulmekki, A. Touache, N. El Moudden, M. Charroud, D. Eliche-Quesada, O. Kizinievic, V. Kizinievic, Recycling argan nut shell and wheat straw as a porous agent in the production of clay masonry units, *Constr. Build. Mater.* 384 (2023), 131369.
- [30] M. Arsenović, S. Stanković, L. Pezo, L. Mančić, Z. Radojević, Optimization of the production process through response surface method: Bricks made of loess, *Ceram. Int.* 39 (3) (2013) 3065–3075.
- [31] M. Arsenović, S. Stanković, Z. Radojević, L. Pezo, Prediction and fuzzy synthetic optimization of process parameters in heavy clay brick production, *Ceram. Int.* 39 (2) (2013).
- [32] M. Arsenović, Z. Radojević, Ž. Jakšić, L. Pezo, Mathematical approach to application of industrial wastes in clay brick production—Part II: Optimization, *Ceram. Int.* 41 (3) (2015) 4899–4905.
- [33] C. Panagiotopoulou, S. Tsivilis, G. Kakali, Application of the Taguchi approach for the composition optimization of alkali activated fly ash binders, *Constr. Build. Mater.* 91 (2015) 17–22.
- [34] F. Anjum, A. Ghaffar, Y. Jamil, M.I. Majeed, Effect of sintering temperature on mechanical and thermophysical properties of biowaste-added fired clay bricks, *J. Mater. Cycles Waste Manage.* 21 (3) (2019) 503–524.
- [35] Y. Zhang, H. Ni, S. Lv, X. Wang, S. Li, J. Zhang, Preparation of sintered brick with aluminum dross and optimization of process parameters, *Coatings* 11 (9) (2021) 1039.
- [36] L. Zhang, Production of bricks from waste materials—A review, *Constr. Build. Mater.* 47 (2013) 643–655.
- [37] L. Pezo, M. Arsenović, Z. Radojević, ANN model of brick properties using LPNORM calculation of minerals content, *Ceram. Int.* 40 (7) (2014) 9637–9645.
- [38] A. Kairakbaev, E. Abdrahimova, V. Abdrahimov, Effect of high-alumina nanotechnogenic petrochemical wastes on the heat resistance of clinker brick, *Glas. Ceram.* 72 (9) (2016) 335–340.
- [39] G. Goel, A.S. Kalamdhad, A. Agrawal, Parameter optimisation for producing fired bricks using organic solid wastes, *J. Clean. Prod.* 205 (2018) 836–844.
- [40] S. Lawanwadeekul, T. Otsuru, R. Tomiku, H. Nishiguchi, Thermal-acoustic clay brick production with added charcoal for use in Thailand, *Constr. Build. Mater.* 255 (2020), 119376.
- [41] M. Priyadarshini, J.P. Giri, M. Patnaik, Variability in the compressive strength of non-conventional bricks containing agro and industrial waste, *Case Stud. Constr. Mater.* 14 (2021) e00506.
- [42] N.H. Zulkernain, P. Gani, C.C. Ng, T. Uvarajan, Optimisation of mixed proportion for cement brick containing plastic waste using response surface methodology (RSM), *Innovat. Instruct. Solut.* 7 (2) (2022) 1–24.
- [43] A. Konak, D.W. Coit, A.E. Smith, Multi-objective optimization using genetic algorithms: A tutorial, *Reliab. Eng. Syst. Saf.* 91 (9) (2006) 992–1007.
- [44] H. Tamaki, H. Kita, and S. Kobayashi, *Multi-objective optimization by genetic algorithms: A review*, in: *Proceedings of IEEE international conference on evolutionary computation*. 1996. IEEE.
- [45] Y. Gao, L. Shi, P. Yao, *Study on multi-objective genetic algorithm*, in: *Proceedings of the 3rd World Congress on Intelligent Control and Automation (Cat. No. 00EX393)*. 2000. IEEE.
- [46] W. Wang, R. Zmeureanu, H. Rivard, Applying multi-objective genetic algorithms in green building design optimization, *Build. Environ.* 40 (11) (2005) 1512–1525.
- [47] Y. Schwartz, R. Raslan, D. Mumovic, Implementing multi objective genetic algorithm for life cycle carbon footprint and life cycle cost minimisation: A building refurbishment case study, *Energy* 97 (2016) 58–68.
- [48] M. Ilbeigi, M. Ghomeishi, A. Dehghanbanadaki, Prediction and optimization of energy consumption in an office building using artificial neural network and a genetic algorithm, *Sustain. Cities Soc.* 61 (2020), 102325.
- [49] Y. Xu, Building performance optimization for university dormitory through integration of digital gene map into multi-objective genetic algorithm, *Appl. Energy* 307 (2022), 118211.
- [50] R.T. Marler, J.S. Arora, Survey of multi-objective optimization methods for engineering, *Struct. Multidiscip. Optim.* 26 (2004) 369–395.
- [51] T.M. Tritt, Thermal conductivity: theory, properties, and applications, Springer Science & Business Media, 2005.
- [52] Y. Han, C. Li, C. Bian, S. Li, C.-A. Wang, Porous anorthite ceramics with ultra-low thermal conductivity, *J. Eur. Ceram. Soc.* 33 (13–14) (2013) 2573–2578.
- [53] M.V. Madurwar, R.V. Ralegaonkar, S.A. Mandavgane, Application of agro-waste for sustainable construction materials: A review, *Constr. Build. Mater.* 38 (2013) 872–878.
- [54] A. C00–, Standard test methods for apparent porosity, water absorption, apparent specific gravity, and bulk density of burned refractory brick and shapes by boiling water, West Conshohocken PA, 2015, pp. 1–3.
- [55] C. Astm, 67–03, Standard test methods for sampling and testing brick and structural clay tile, American Society for Testing and Materials, Philadelphia, PA, 2003.
- [56] N. Kucukdogan, L. Aydin, M. Sutcu, Theoretical and empirical thermal conductivity models of red mud filled polymer composites, *Thermochim Acta* 665 (2018) 76–84.
- [57] L. Aydin, H.S. Artem, and S. Oterkus, *Designing engineering structures using stochastic optimization methods*. 2020: CRC Press, Taylor & Francis Group.
- [58] F. Anjum, M. Naz, A. Ghaffar, S. Shukrullah, N. AbdEl-Salam, K. Ibrahim, Study of thermal and mechanical traits of organic waste incorporated fired clay porous material, *Phys. B Condens. Matter* 599 (2020), 412479.
- [59] S. Ozturk, M. Sutcu, L. Aydin, O. Gencel, Thermal Optimization of Lightweight and Micro-porous Clay Bricks for Building Applications, in: *Designing Engineering Structures Using Stochastic Optimization Methods*, CRC Press, 2020, pp. 217–225.
- [60] A. Yaras, Combined effects of paper mill sludge and carbonation sludge on characteristics of fired clay bricks, *Constr. Build. Mater.* 249 (2020), 118722.
- [61] D. Eliche-Quesada, M. Felipe-Sesé, J. López-Pérez, A. Infantes-Molina, Characterization and evaluation of rice husk ash and wood ash in sustainable clay matrix bricks, *Ceram. Int.* 43 (1) (2017) 463–475.
- [62] A. C90, *Standard Specification for Loadbearing Concrete Masonry Units*. Annual book of ASTM standards, United States, 2014.
- [63] P. Muñoz, M. Mendivil, V. Letelier, M. Morales, Thermal and mechanical properties of fired clay bricks made by using grapevine shoots as pore forming agent. Influence of particle size and percentage of replacement, *Constr. Build. Mater.* 224 (2019) 639–658.
- [64] A. Viani, G. Cultrone, K. Sofriadiis, R. Ševcík, P. Šásek, The use of mineralogical indicators for the assessment of firing temperature in fired-clay bodies, *Appl. Clay Sci.* 163 (2018) 108–118.
- [65] G. Cultrone, F.J.C. Rosua, Growth of metastable phases during brick firing: Mineralogical and microtextural changes induced by the composition of the raw material and the presence of additives, *Appl. Clay Sci.* 185 (2020), 105419.